Crystalline Structure and Morphology of Poly(L-lactide) Formed under High-Pressure CO_2

Hironori Marubayashi, Satoshi Akaishi, Shuichi Akasaka, Shigeo Asai,* and Masao Sumita

Department of Chemistry and Materials Science, Tokyo Institute of Technology, Ookayama, Meguro, Tokyo 152-8552, Japan

Received April 5, 2008; Revised Manuscript Received August 14, 2008

ABSTRACT: Crystalline structure and morphology of poly(L-lactide) (PLLA) formed under high-pressure CO_2 were studied by comparing the CO_2-treated PLLA and the annealed one in terms of the crystallization behavior, crystalline forms, and crystalline superstructures. The crystallization temperature dependence of the diffraction peak position ($2\theta \approx 16°$) and crystallinity for the CO_2-treated PLLA indicates that the crystal modification changes continuously from the disorder α (α″) to α forms not through the α′ one with increasing temperature. By using light scattering technique, we clarified that the morphological transition from spherulites on a micrometer scale to rodlike crystalline superstructures on a nanometer scale occurs around 15 °C under 7−15 MPa CO_2 and around 30 °C under 3 MPa CO_2. By introducing the parameters η and Δ in the theoretical calculation for Vv light scattering from spherulites, it is indicated that there is a distinct difference in the arrangement of crystalline lamellae within spherulite between the CO_2-treated PLLA and the annealed one.

Introduction

Nowadays, mass production, consumption, and disposal of petroleum-based polymeric materials in a short period of time cause several crucial problems. Because of dependence on a finite fossil fuel, there is an essential problem inherent in the heavy use of petroleum-based polymeric materials: exhaustion of the raw material in the near future. In terms of the problems occurring after use, incineration disposal of the petroleum-based polymeric materials results in the emission of carbon dioxide, which is one of the greenhouse gases, while there are few landfills left because of their very poor biodegradability. Therefore, alternatives to the petroleum-based polymeric materials are extremely needed for sustainable life. In response to such problems with great urgency, "biobased polymer" attracts more and more attention because this kind of polymer can be synthesized from renewable natural resources, that is, has carbon neutrality. Various biobased polymers have been extensively studied in terms of structure and properties. Poly(L-lactide) (PLLA), one of the enantiomers of polylactide, can be synthesized from plant-derived materials. Since PLLA is a semicrystalline polymer with a relatively low crystallization rate, the amorphous sample with high transparency can be obtained by quenching from the molten state, which is unusual among the biobased polymers. Depending on the crystallization condition, PLLA forms several types of crystalline modifications: the α,[1,2] β,[2,3] and γ forms.[4] Furthermore, another crystalline modification, the α′ (disorder α) form, was studied by many researchers recently.[5−12] The α′ crystals are formed by the crystallization below 100 °C, while the α ones are developed by the crystallization above 120 °C.[7,9−11] On the basis of the X-ray fiber diagram and polarized IR/Raman spectra, Zhang et al. proposed that the chain conformation and chain packing mode of the α′ form are slightly different from those of the α form of PLLA.[6] Kawai et al. reported that the α′ form has a hexagonal packing, because the ratio of the *a*- and *b*-axis lengths is $3^{1/2}$ and the absence of some diffractions is well explained by the extinction rule of the hexagonal lattice.[9] Pan et al. found that the α′ crystals in low molecular weight PLLA only partially transform into the α ones, and some amounts of α′ ones melt directly without transition during the heating process, while almost all of the α′ ones in high molecular weight PLLA transform into the α ones in the heating scan.[10] They also showed that the melting of PLLA with various molecular weights changes from the phase transition (α′-to-α) + melting mechanism to the usual melt−recrystallization mechanism with increasing the crystallization temperature (T_c). The lattice parameters *a* and *b* of the PLLA α′ form are different from those of the α form, while there is no difference in the lattice parameter *c* between the α′ and α forms.[9,11] Yasuniwa et al. showed that the multiple melting behavior of PLLA is due to the increase in crystallinity through melt−recrystallization because of the increase in the X-ray diffraction intensity before final melting.[12] In terms of the crystalline morphology for PLLA, spherulites with negative birefringence are grown by crystallization from the melt or solution, which is attributed to the fact that PLLA chains are oriented in the direction perpendicular to the radial direction of spherulites.[8,13−15]

Although concentrated only on the negative aspects as the greenhouse gas, CO_2 attracts much attention as the environmentally friendly solvent because of its characteristics of safety and easy removal from polymer matrix (i.e., generation of no liquid toxic waste, unlike the conventional organic solvents). Furthermore, relatively moderate critical condition ($P_{critical}$ = 7.38 MPa and $T_{critical}$ = 31.1 °C) and low cost support the widespread use of CO_2. In polymer processing, there is a strong possibility of preparation of the novel polymeric materials of high value by using CO_2 as plasticizing agents, foaming agents, and so forth.[16] By using CO_2 as a plasticizing agent for semicrystalline polymer, the depression in the glass transition temperature (T_g)[17,18] and melting temperature (T_m)[18] occurs because of the plasticizing effect of CO_2 similar to that of the organic solvents,[19] which leads to the crystallization below original T_g,[20−24] changes in the crystallization rate,[21,22,25−28] and formation of the unique crystalline morphology.[29] Depending on the CO_2 treatment conditions and resulting T_g and T_m depression of polymer, the crystallization rate increases in some cases[21,22,25] and decreases in other cases.[26−28] Handa et al. reported that there are transitions between various crystalline forms that only occur in the presence of CO_2 in syndiotactic

* To whom all correspondence should be addressed. Tel.: +81-3-5734-2432. Fax: +81-3-5734-2431. E-mail: asai.s.aa@m.titech.ac.jp.

10.1021/ma800766h CCC: $40.75
Published on Web 11/07/2008

polystyrene (sPS).[22] Asai et al. revealed that the crystallite size of poly(ethylene 2,6-naphthalate) decreases with decreasing the CO_2 treatment temperature.[23] Hirota et al. reported that PLLA/poly(methyl methacrylate) (PMMA) blends can be crystallized even at a low temperature of 0 °C under high-pressure CO_2.[24] Furthermore, it was indicated that the size of PLLA crystals in the CO_2-treated PLLA/PMMA film is smaller than the wavelength of the visible light because of its good transparency. With respect to the crystallization kinetics under CO_2, Takada et al. reproduced the overall crystallization rate of PLLA under CO_2 taking into consideration the depression in T_g and equilibrium melting temperature.[25−27] Oda and Saito pointed out that crystallization kinetics under CO_2 differs from that in air and the exclusion effect of CO_2 from the crystal growth front needs to be considered.[28] In terms of the morphology control using CO_2, Teramoto et al. reported that the various crystalline morphology of polypropylene is obtained by melt crystallization under CO_2.[29]

PLLA crystals formed under high-pressure CO_2 at 0 °C were found to be disordered compared with those formed in air based on the broad X-ray diffraction peak.[24] However, a detailed investigation on the crystallization behavior and crystalline forms of PLLA treated with high-pressure CO_2 has not been conducted yet. Furthermore, the relationship between high transparency and higher-order structure of the CO_2-treated PLLA has not been clarified. In general, the hierarchical structure consisting of crystalline lamella such as spherulites, which is described as the "crystalline superstructure" in this article, has a great effect on the macroscopic material properties such as the transparency of a film and mechanical properties. To investigate the crystalline superstructure of the CO_2-treated PLLA, we used the light scattering technique, which is a powerful tool to characterize the structure on the scale from submicrometer to micrometer such as spherulites,[30−33] rodlike crystals,[30,34−37] and sheaflike crystals.[30,38,39] In this article, we conducted comparative studies on the CO_2-treated PLLA and the annealed one in terms of the crystallization behavior, crystalline forms, and crystalline superstructures as functions of CO_2 pressure and temperature using differential scanning calorimetry (DSC), wide-angle X-ray diffraction (WAXD), and light scattering methods, respectively. Furthermore, the relationship between the crystalline superstructure and high transparency of the CO_2-treated PLLA was examined.

Experimental Section

Film Preparation. PLLA pellets (Lacty #5000, $M_w = 320\,000$) were supplied by the Toyota Motor Corporation. The amorphous film with a thickness of 0.2 mm was obtained by melt pressing the pellets at 180 °C and 20 MPa for 5 min and subsequent quenching into ice water. To remove water, the resultant film was dried under vacuum at room temperature for ca. 1 day. The amorphous film obtained has high transparency.

The annealed films were prepared by annealing the amorphous films in air at the constant temperature in the temperature range from 65 to 140 °C for 2 h using a FP900 Thermo System (Mettler-Toledo International, Inc.) and subsequent quenching into liquid nitrogen. In addition, to complete the crystallization of PLLA, the annealing periods at 65, 70, and 75 °C were set to 300, 50, and 10 h, respectively.

To prepare the CO_2-treated films, the amorphous films were placed into a pressure vessel and exposed to high-pressure CO_2 under the desired pressures from 3 to 15 MPa and the desired temperatures from 0 to 70 °C for 2−20 h using CO_2 treatment system (JASCO Corporation), as described in detail elsewhere.[23,24] After the CO_2 treatment, the vessel was depressurized from 10 MPa to atmospheric pressure, and subsequently the films were taken out of the vessel. Not only to remove remaining CO_2 in the films but also to avoid some structural changes in the plasticized state including CO_2, the resultant films were kept at low temperature, 5 °C, in air for 3 days and subsequently dried under vacuum at room temperature for 1 week.

Differential Scanning Calorimetry. DSC measurements were carried out using a DSC-50 (Shimadzu Corporation) in the temperature range from room temperature to 200 °C at a heating rate of 10 °C/min under a nitrogen gas atmosphere. The degree of crystallinity (χ_{c_DSC}) for each PLLA film was calculated from the following equation:

$$\chi_{c\_DSC} = \frac{\Delta H_m - \Delta H_c}{\Delta H_m^0} \times 100 \quad (1)$$

where ΔH_m^0 is the heat of fusion for the perfectly crystalline PLLA (85.82 J/g), ΔH_m is the heat of fusion for PLLA during a DSC heating run, and ΔH_c is the heat of crystallization for PLLA during a DSC heating run.

Wide-Angle X-ray Diffraction. WAXD measurements were carried out using a RINT-2100 system (Rigaku Corporation) with Cu Kα radiation ($\lambda = 0.15418$ nm) operating at 40 kV and 40 mA in the diffraction angle range between 3 and 60°. The system was equipped with a graphite monochromator and a scintillation counter. The degree of crystallinity (χ_{c_WAXD}) for each PLLA film was calculated from the following equation:

$$\chi_{c\_WAXD} = \frac{\int_{2\theta_1}^{2\theta_2} I_c(2\theta)\, d(2\theta)}{\int_{2\theta_1}^{2\theta_2} I(2\theta)\, d(2\theta)} \times 100 \quad (2)$$

where the values of $2\theta_1$ and $2\theta_2$ used in this study are 5 and 40°, respectively, $I_c(2\theta)$ is the diffraction intensity from the crystalline phase, and $I(2\theta)$ is the diffraction intensity from both the crystalline and amorphous phases.

Light Scattering. Light scattering measurements were carried out using a DYNA-3000 (Otsuka electronics Co., Ltd.) with a 5 mW He−Ne laser ($\lambda = 632.8$ nm) as a light source. To estimate both the fluctuation in optical anisotropy and that in density derived from the crystalline superstructure of the CO_2-treated PLLA, measurements were conducted in both Hv and Vv polarization. Both polarizer and analyzer were set in vertical direction for Vv polarization, while polarizer and analyzer were set in vertical and horizontal directions, respectively, for Hv polarization. The Hv light scattering was caused only by the fluctuation in optical anisotropy, while the Vv light scattering was brought about by both the fluctuations in optical anisotropy and density.[30] Therefore, by combining Hv and Vv polarization, information about the fluctuation in optical anisotropy and that in density could be estimated separately. After being polarized in vertical direction through the vertical polarizer, a He−Ne laser was scattered by the fluctuations in optical anisotropy and density derived from the crystalline superstructure in a film and subsequently only the component of the incident and scattered lights parallel to the analyzer was detected by CCD camera with 128 × 128 pixels. The light scattering derived from microasperity of a film surface was minimized by sandwiching a film between glass plates with silicon oil.

To evaluate the radius of spherulite for the films showing "four-leaf-clover" pattern in Hv polarization, the one-dimensional scattering profile (intensity vs θ_0) was obtained by subtraction of the scattering profile at azimuthal angle $\mu = 0°$ from that at $\mu = 45°$ and subsequent simplification of the resultant scattering profile using fourth-order Fourier series, taking into consideration the μ independent scattering (circularly symmetric scattering) with relatively low intensity in small-angle region and poor signal-to-noise ratio, respectively. Furthermore, to estimate the scattering angle in a film accurately, the one-dimensional scattering profiles obtained (intensity vs θ_0) were corrected by Snell's law, taking into account the refraction in some boundaries through which the scattered light passed: film−oil, oil−glass, and glass−air boundaries. In case of the traveling of light in multiple layers (film, oil, glass, and air), the final traveling direction of light, which corresponds to the

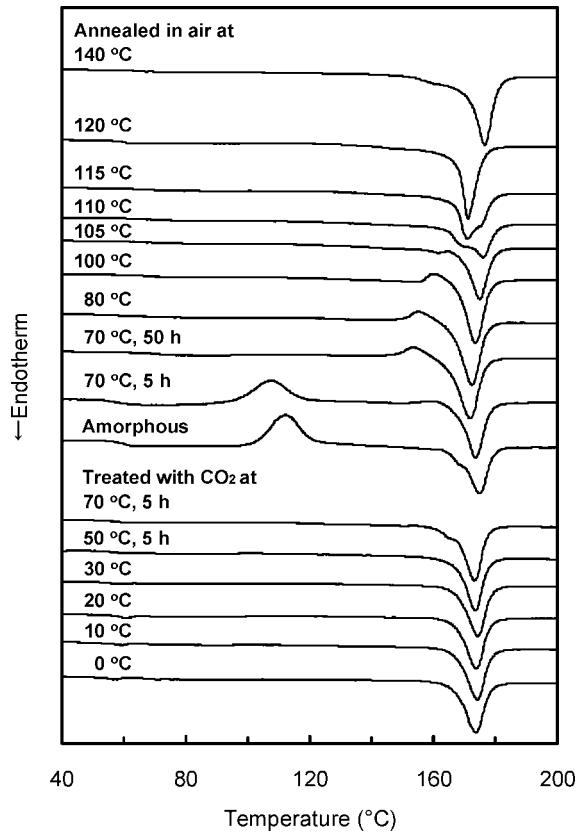

Figure 1. DSC curves of the CO_2-treated films (10 MPa) and annealed ones. The CO_2 treatments and annealing in air without labeling of the crystallization time were conducted for 2 h.

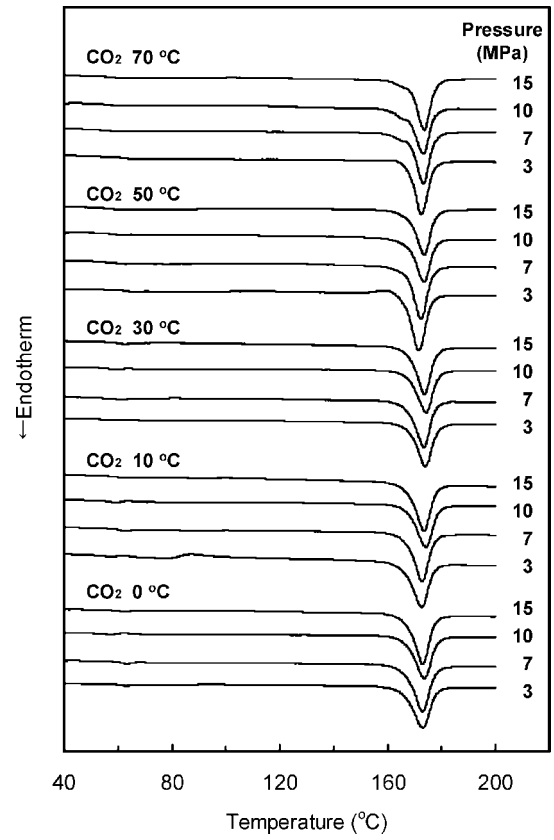

Figure 2. DSC curves of the PLLA films crystallized at various CO_2 pressure levels. The CO_2 treatments under 3−15 MPa at 0−40 °C were conducted for 2 h. The CO_2 treatments under 3−15 MPa at 50−70 °C were conducted for 5 h.

scattering angle measured (θ_0), was determined only by the exterior mediums (film and air). Accordingly, the scattering angle in a film (θ) is given by

$$n \sin \theta = n_0 \sin \theta_0 \tag{3}$$

where n is the refractive index of a PLLA film (1.45), which is the measured value at a wavelength of 589 nm by an Abbe refractometer, and n_0 is the refractive index of air (1.00). Finally, the average radius of spherulite (R) in a film was calculated from[30−33]

$$\frac{4\pi nR}{\lambda} \sin\left(\frac{\theta_m}{2}\right) = 4.09 \tag{4}$$

where λ is the wavelength of the laser (0.6328 μm) and θ_m is a scattering peak position in the corrected one-dimensional scattering profile (intensity vs θ).

Results and Discussion

Crystallization Behavior and Crystalline Forms of CO_2-Treated PLLA. First, DSC curves of the PLLA films treated with CO_2 under 10 MPa at 0−70 °C compared with those of the amorphous and annealed films are shown in Figure 1. It was confirmed that no crystallization occurs by the annealing in air at 70 °C for 5 h, because the DSC curve of the corresponding film was almost the same as that of the amorphous film, in which the exothermic peak around 110 °C and the endothermic one around 175 °C with equivalent peak area were observed. These exothermic and endothermic peaks are attributed to the crystallization and melting of PLLA during the DSC heating run, respectively. For the annealing in air at 70 °C, it took 50 h for PLLA to crystallize sufficiently. In contrast, the exothermic peak around 110 °C was not observed for the films annealed in air at 80−140 °C for 2 h, showing the sufficient crystallization of PLLA by the annealing in air in this temperature range. Thus, it requires the temperature of 80 °C and over to complete the crystallization of PLLA within 2 h. The small exothermic peak at 150−165 °C just before the melting endothermic one around 175 °C, which was observed for the films annealed in air at 80−100 °C, is attributed to the crystalline transition from the α′(disorder α) to α forms, as reported previously.[7,9−12] The films annealed in air at 105−115 °C showed the double melting peaks, while the films annealed in air at 80−100 °C and 120−140 °C exhibited the single melting peak at a heating rate of 10 °C/min. Yasuniwa et al. reported that, when T_c is lower than 135 °C, PLLA shows the double melting behavior during the DSC heating run at 10 °C/min.[40]

On the other hand, the films treated with 10 MPa CO_2 at 0−40 °C for 2 h and at 50−70 °C for 5 h exhibited only the endothermic peak around 175 °C (i.e., sufficient crystallization occurred, while no crystallization occurred for the annealing in air below 70 °C for 5 h). It is attributed to the depression in T_g from the original value (ca. 60 °C) to the temperature much lower than the CO_2 treatment temperature due to the plasticizing effect of CO_2.[17,18,20−27] In addition, the small exothermic peak before melting was not observed for the CO_2-treated PLLA films (10 MPa), implying that the PLLA crystals formed under CO_2 are different from those formed in air below 100 °C (the α′ form), as mentioned later using WAXD data. In terms of the CO_2 temperature dependence of DSC curves, the films treated with 10 MPa CO_2 at 0−50 °C showed the single melting peak, whereas those treated with 10 MPa CO_2 at 60−70 °C exhibited the double melting peak. Thus, the T_c dependence of the melting behavior for the CO_2-treated PLLA is smaller than that for the annealed PLLA.

Second, Figure 2 shows the CO_2 pressure dependence of DSC curves for several CO_2-treated films. There was almost no CO_2

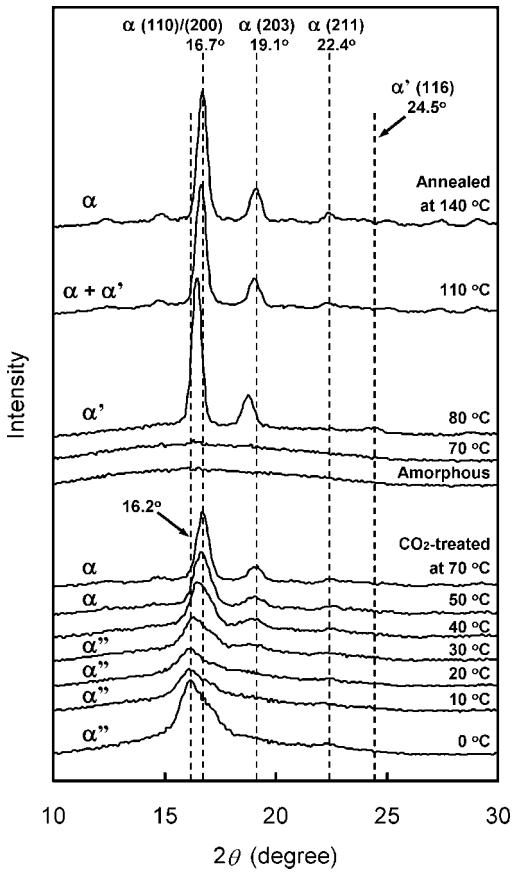

Figure 3. WAXD profiles of the CO_2-treated films (10 MPa) and annealed ones. The CO_2 treatments under 10 MPa at 0−40 °C and annealing in air at 80−140 °C were conducted for 2 h. The CO_2 treatments under 10 MPa at 50−70 °C and annealing in air at 70 °C were conducted for 5 h.

pressure dependence in DSC curves for the CO_2 treatments at 0, 30, and 40 °C. In contrast, the PLLA films crystallized under 3 MPa CO_2 at 10−20 °C showed the small exothermic peak around 85−90 °C, whereas those crystallized under 7−15 MPa CO_2 in the same temperature range showed only the endothermic melting peak. This small exothermic peak remained and kept the peak area even after the CO_2 treatment for 10 h, implying that the crystallization of PLLA is not completed under 3 MPa CO_2 at 10−20 °C. For the CO_2 treatments at 50−70 °C, there was the CO_2 pressure dependence in melting behavior. The films treated with 3 MPa CO_2 at 50−60 °C showed the small exothermic peak before melting, while those treated with 7−15 MPa CO_2 in the same temperature range showed only the melting peak. The small exothermic peak observed for the CO_2 treatment under 3 MPa at 50 °C disappeared by extending the treatment time from 5 to 20 h, while that for the CO_2 treatment under 3 MPa at 60 °C remained and kept the peak area even after the CO_2 treatment for 20 h. Furthermore, the film treated with 3 MPa CO_2 at 70 °C showed the single melting peak, while those treated with 7−15 MPa CO_2 at 70 °C showed the double melting peaks. Thus, it was found that the melting behavior of PLLA shows relatively small changes with the CO_2 pressure and temperature.

Figure 3 shows WAXD profiles of the PLLA films treated with CO_2 under 10 MPa at 0−70 °C compared with those of the amorphous and annealed films. A sharp diffraction peak was observed around $2\theta = 16°$ for the films annealed in air at 80−140 °C for 2 h, whereas an amorphous halo was observed for the film annealed in air at 70 °C for 5 h. The diffraction peak position was $2\theta = 16.7°$ (the α form) for the films annealed in air at 120−140 °C, while 16.5° (the α′ form) for the films annealed in air below 100 °C, in agreement with previous studies[1,2,5−12] and DSC results mentioned above. For the annealed PLLA (105−115 °C), the diffraction peak was located around $2\theta = 16.6°$, an intermediate value of 16.5° (the α′ form) and 16.7° (the α form). Thus, WAXD and DSC results show that no crystallization occurs during the annealing in air at 70 °C for 5 h and the crystalline transition from the α′ to α forms occurs around 110 °C. In contrast, several diffraction peaks were observed for the films treated with 10 MPa CO_2 at 0−40 °C for 2 h and at 50−70 °C for 5 h, indicating the occurrence of CO_2-induced crystallization of PLLA, which is in agreement with DSC results mentioned above. WAXD profiles of the CO_2-treated PLLA films were significantly broader than those of the annealed ones. The peak intensity of the CO_2-treated PLLA decreased with decreasing CO_2 treatment temperature at 5−70 °C, although almost no changes were observed in the corresponding DSC curves (Figure 1). Since the crystallinity of the CO_2-treated films calculated from DSC curves had an almost constant value as mentioned later, this broadening of the diffraction peaks around 16 and 19° with decreasing temperature implies that the crystalline regularity on the unit cell scale decreases with decreasing CO_2 treatment temperature.

In WAXD profiles of the films treated with 10 MPa CO_2 at 0−30 °C, a broad diffraction peak was located at $2\theta = 16.1-16.3°$, which obviously differs from the (110)/(200) reflections of the α form ($2\theta = 16.7°$)[1,2] and the α′ one ($2\theta = 16.5°$).[5−12] In contrast, for the films treated with CO_2 under 10 MPa at 50−70 °C, strong diffraction peaks were observed at $2\theta = 16.7$ and 19.1°, which are attributed to the (110)/(200) and (203) reflections of the α form, respectively.[1,2] In addition, for the films treated with 10 MPa CO_2 at 40 °C, a broad diffraction peak was located at $2\theta = 16.6°$ and a diffraction peak around $2\theta = 19°$ started to appear. As reported previously, a relatively small diffraction peak at $2\theta = 24.5°$ is observed only in the α′ form,[5−11] whereas a relatively weak diffraction peak at $2\theta = 22.4°$ appears only in the α form.[1,2,5−11] All the CO_2-treated films showed only the latter diffraction peak, although the signal-to-noise ratio was relatively low. This result clearly shows that the crystal modification of the CO_2-treated PLLA is different from the α′ form ($2\theta = 16.5$, 18.9, and 24.5°).[5−12] Here, we define the crystal modification of the PLLA treated with 10 MPa CO_2 at 0−30 °C ($2\theta = 16.1-16.3°$) as the α″ form, which is distinctly separated from the α form[1,2] or α′ form,[5−12] although the α″ and α′ forms are equivalent in terms of the disordered α form. Figure 4 displays the CO_2 pressure dependence of WAXD curves for the CO_2-treated films. For the PLLA treated with CO_2 at 0, 10, 20, and 40 °C, there was almost no CO_2 pressure dependence in the diffraction intensity and peak positions of WAXD curves. On the other hand, for the PLLA treated with CO_2 at 30, 50, 60, and 70 °C, the diffraction peak positions changed with increasing pressure from 3 to 7 MPa. The peak positions for the film crystallized under 3 MPa CO_2 at 30 °C were 16.6 and 19.0°, while that for the films treated with CO_2 under 7−15 MPa at 30 °C was 16.3° (the α″ form). For the CO_2-treated PLLA (50−70 °C), the peak positions shifted from $2\theta = 16.6$ and 19.0° to $2\theta = 16.7$ and 19.1° (the α form) with increasing pressure from 3 to 7 MPa. In summary, it was clarified that PLLA molecules in the compressed CO_2 form the α″ crystals under 3−15 MPa at 0−20 °C and under 7−15 MPa at 30 °C, whereas the α crystals are formed under 7−15 MPa at 50−70 °C, as shown in Figure 5.

The peak position at $2\theta = 16.1-16.3°$ for the α″ form indicates that the *d*-spacing of (200)/(110) planes for the α″ form is larger than that for the α′ ($2\theta = 16.5°$) or α form ($2\theta = 16.7°$). Namely, the α″ form is considered to have poor chain packing and lower crystal density compared with that of the α′ or α form. The peak shifting from $2\theta = 16.1-16.3°$ to the

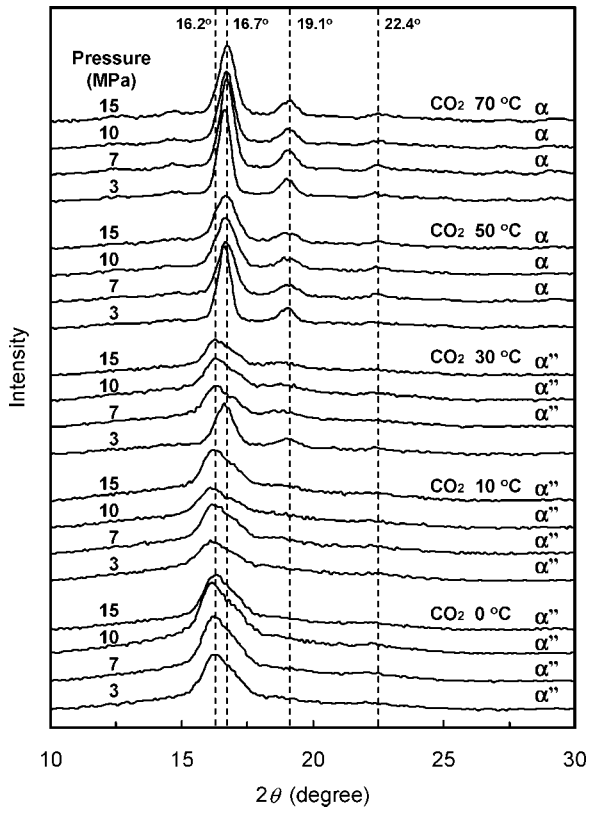

Figure 4. WAXD curves of the PLLA films crystallized at various CO_2 pressure levels. The CO_2 treatments under 3−15 MPa at 0−40 °C were conducted for 2 h. The CO_2 treatments under 3−15 MPa at 50−70 °C were conducted for 5 h.

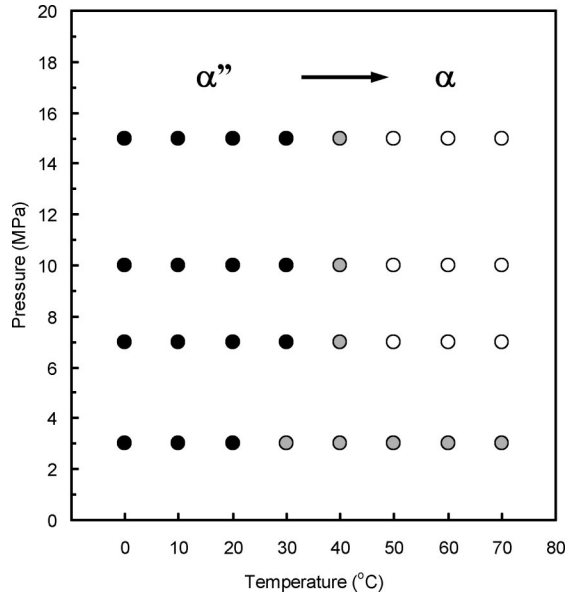

Figure 5. Phase diagram of crystalline structure of the CO_2-treated PLLA. Black, gray, and white circles represent the α″ form (2θ = 16.1−16.3°), intermediate crystalline structure between the α″ and α ones (2θ = 16.6°), and the α one (2θ = 16.7°), respectively.

higher diffraction angle and appearance of other crystalline reflections (e.g., $2\theta \approx 19°$) with increasing temperature imply that the chain packing becomes compact and crystalline order increases with T_c.

As one of the possible mechanisms of such an increase in the *d*-spacing of (200)/(110) planes, we assume the inclusion of CO_2 in the unit cell of PLLA. Our hypothesis is that the

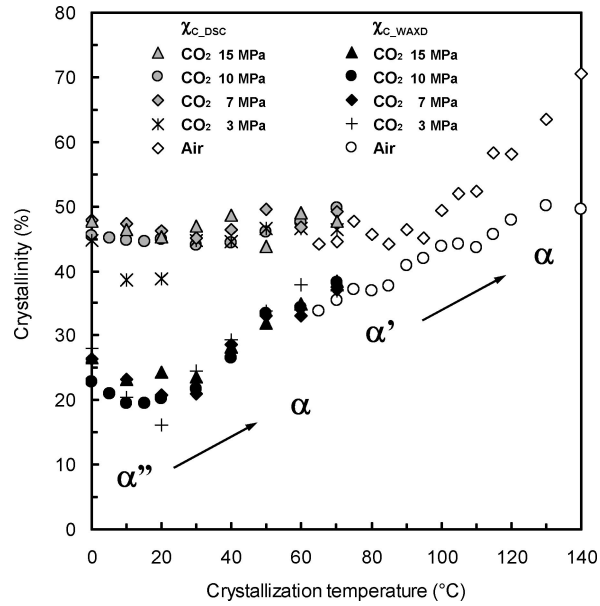

Figure 6. Degree of crystallinity for the CO_2-treated films and annealed ones. The CO_2 treatments under 3−15 MPa at 0−40 °C and annealing in air at 80−140 °C were conducted for 2 h. The CO_2 treatments under 3−15 MPa at 50−70 °C were conducted for 5 h. The annealing periods at 65, 70, and 75 °C were 300, 50, and 10 h, respectively.

PLLA α form is expanded by the inclusion of a certain amount of CO_2 molecules during CO_2-induced crystallization and when CO_2 molecules are removed from the film, the place that had been occupied by CO_2 molecules remains as cavities, as is the case with the δ_e (empty δ) form of sPS.[41] To verify our hypothesis, in situ WAXD measurements during the high-pressure CO_2 treatment remain to be conducted.

Next, we discuss the origin of disorder in the unit cell for the CO_2-treated PLLA showing broader WAXD curves compared with those of the annealed PLLA. In CO_2-induced crystallization, CO_2 that plasticizes polymer is excluded from the crystalline region of polymer, as proposed by Oda, Koga, and Saito.[28,42] With decreasing CO_2 treatment temperature, more CO_2 molecules are required to reduce T_g of polymer to the temperature lower than the CO_2 treatment temperature for crystallization. Therefore, more CO_2 molecules should be excluded from the lamella during crystallization with decreasing CO_2 treatment temperature, resulting in the enhancement of structural disorder. Namely, the increase in the degree of disorder in the crystalline structure with decreasing temperature (the α−α″ transition) might be attributed to the increase in the degree of CO_2 exclusion.

Crystallinity and Melting Temperature of CO_2-Treated PLLA. The degree of crystallinity for the CO_2-treated PLLA films and annealed ones calculated from DSC and WAXD curves (described as χ_{c_DSC} and χ_{c_WAXD}, respectively) is displayed in Figure 6. The melting temperature (T_m) of the CO_2-treated PLLA films and annealed ones determined from DSC curves (Figures 1 and 2) is shown in Figure 7. Since PLLA annealed in air at 105−115 °C showed the double melting behavior as mentioned above, lower T_m and the higher one are defined as T_{m_low} and T_{m_high}, respectively. As represented by the Thomson−Gibbs equation, T_m increases with increasing lamellar thickness.[43] In general, there is considered to be uncertainty inherent in χ_{c_DSC} because of difficulty to obtain the heat of fusion of the completely crystallized polymer (ΔH_m^0) definitely.[44,45] Various values of ΔH_m^0 of PLLA have been reported by several researchers: 81.3−93.0 J/g,[13,46,47] 106 J/g,[48] and 142−148 J/g.[49] In this study, we used a value of 85.82 J/g

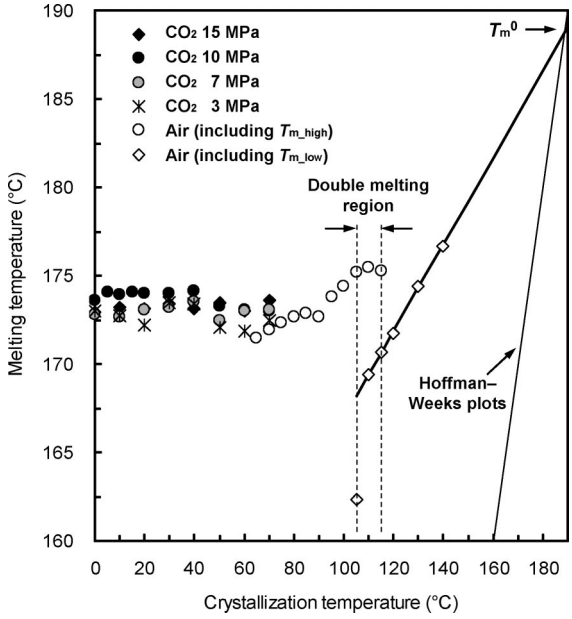

Figure 7. Melting temperature of the CO_2-treated films and annealed ones. The CO_2 treatments under 3−15 MPa at 0−40 °C and annealing in air at 80−140 °C were conducted for 2 h. The CO_2 treatments under 3−15 MPa at 50−70 °C were conducted for 5 h. The annealing periods at 65, 70, and 75 °C were 300, 50, and 10 h, respectively.

as the ΔH_m^0, which was obtained by plotting the heat of fusion (ΔH_m) against the χ_{c_WAXD} followed by regression using the straight line passing through zero point (i.e., the slope of the regression line corresponds to ΔH_m^0). In general, χ_{c_WAXD} is considered to be smaller than the weight fraction crystallinity calculated from density, because the crystalline diffraction intensity is lost by thermal vibrations and crystal imperfections.[45] That is, χ_{c_WAXD} can be regarded as the crystallinity more sensitive to the crystalline regularity compared with that obtained by other methods.

For the films annealed in air, χ_{c_DSC} was almost constant at 65−90 °C and increased with increasing temperature at 95−140 °C, as reported previously.[7,47] Simultaneously, χ_{c_WAXD} increased with increasing temperature at 65−130 °C and leveled off (∼50%) at 130 °C, suggesting the increase in crystal regularity with temperature through the α′-to-α transition. As Yasuniwa et al. reported, T_c dependence of T_m for PLLA is complex compared with other semicrystalline polymers because of the double melting behavior and crystal polymorphism.[40] Similar T_c dependence of T_m was confirmed for the annealed PLLA by our DSC results, as shown in Figure 7. The equilibrium melting temperature (T_m^0) obtained by Hoffman−Weeks plots[50] in the temperature range from 110 to 140 °C was 188.7 °C, which is in agreement with that obtained by some researchers previously (187−190 °C),[7,8,27] but lower than that found by others (206−207 °C).[14,47]

For the CO_2-treated PLLA, there was the increase in χ_{c_WAXD} with increasing temperature in spite of almost constant χ_{c_DSC} (44−50%) except for the CO_2 treatments under 3 MPa at 10−20 °C (ca. 38%). This result indicates that the crystal regularity increases with increasing CO_2 treatment temperature through the α″-to-α transition. Such T_c dependence of χ_{c_WAXD} and χ_{c_DSC} for the CO_2-treated films is similar to that of the annealed ones (65−90 °C). However, these changes in χ_{c_WAXD} and χ_{c_DSC} of the CO_2-treated films were accompanied with the crystalline transition from the α″ to α forms, whereas the annealed ones (65−90 °C) exhibited the single crystal modification (the α′ form). As shown in Figure 7, T_m of the CO_2-treated films was in the temperature range between 172 and 174 °C, which is comparable with that of the films annealed below 100 °C. This result can be explained by the development of relatively thick lamellae due to the depression in the degree of supercooling by the plasticizing effect of CO_2.[25−27] Furthermore, T_m of the CO_2-treated films showed no distinct CO_2 pressure and temperature dependence, while the crystalline forms and χ_{c_WAXD} showed a strong T_c dependence. Thus, it was revealed that high-pressure CO_2 treatments even at relatively low temperature enable PLLA molecules to crystallize to the extent comparable with the annealing in air at 65−95 °C (χ_{c_DSC} = 44−50%), although the crystalline regularity of the CO_2-treated PLLA is much lower than that of the annealed one. Here, there is a possibility of the structural changes during heating run, although neither exothermic peaks nor endothermic ones were observed in DSC curves of the CO_2-treated PLLA except for the melting endothermic one. The effect of reannealing on the crystalline forms, crystallinity, and T_m of the CO_2-treated PLLA remains to be investigated.

Crystalline Superstructures of CO_2-Treated PLLA. Figures 8 and 9 show Hv and Vv light scattering patterns of the CO_2-treated PLLA films compared with those of the annealed ones, respectively. The amorphous film and annealed ones (130−140 °C: data are not displayed) showed no distinct light scattering patterns in both Hv and Vv polarization. For the films treated with CO_2 under 7−15 MPa at 20−70 °C, those treated with CO_2 under 3 MPa at 40−70 °C, and those annealed in air at 70−120 °C, the "four-leaf-clover" pattern, in which scattering peaks are located at azimuthal angle μ = 45, 135, 225, 315° (odd multiples of 45°) and at a given scattering angle θ, was observed for Hv polarization (Figure 8). In Vv polarization (Figure 9), scattering peaks were present in vertical direction with twofold symmetry. These light scattering patterns obtained are the characteristic light scattering patterns of spherulites.[30−33] Spherulite is a spherical aggregate of crystallites with different radial and tangential refractive indices that results from the arrangement of the anisotropic crystallites consisting of lamella within spherulite.[31] Such optical anisotropy of spherulite yields the patterns with fourfold and twofold symmetry in Hv and Vv polarization, respectively. The average spherulite radius of the CO_2-treated films and annealed ones, which was calculated from eq 4, is shown in Figure 10. Here, the radius of spherulite for the annealed films (95−120 °C) could not be estimated, because it was difficult to determine the scattering peak position due to overlapping of the "four-leaf-clover" pattern with a beam stop (θ < 3°). Also, for the annealed films (130−140 °C), the scattering-angle range in which the "four-leaf-clover" pattern appears might be too low to be characterized by this light scattering system with a beam stop at θ < 3°. For the annealed films (70−90 °C), the radius of spherulite decreased linearly with decreasing annealing temperature. Similarly, for the CO_2-treated PLLA, the average spherulite radius decreased linearly with decreasing CO_2 treatment temperature regardless of the CO_2 pressure, as shown in Figure 10. At the same T_c, the spherulite radius was almost constant regardless of the CO_2 pressure. Takada et al. proposed the crystallization kinetics model under high-pressure CO_2 based on the depression in T_g and T_m by the plasticizing effect of CO_2.[25−27] In their model, the crystal nucleation rate decreases by the T_m depression (i.e., the depression in the degree of supercooling), while the crystal growth rate increases by the T_g depression (i.e., the increase in the chain mobility). Following their model, we discuss the changes in the spherulite size of PLLA with the CO_2 treatment temperature in terms of the T_g and T_m depression. If the CO_2-induced T_m depression is smaller than the decrease in T_c (i.e., the CO_2 treatment temperature), the degree of supercooling ($T_m - T_c$) increases with decreasing T_c in CO_2-induced crystallization. In this case, the crystal nucleation density increases with

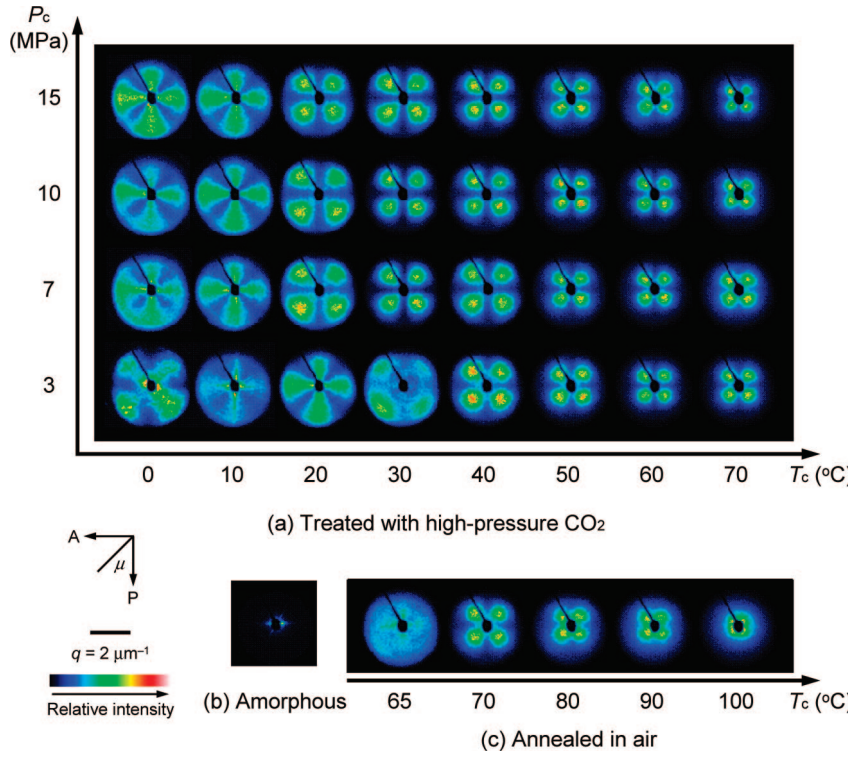

Figure 8. Hv light scattering patterns of the CO_2-treated films and annealed ones. The CO_2 treatments under 3−15 MPa at 0−40 °C and annealing in air at 80−100 °C were conducted for 2 h. The CO_2 treatments under 3−15 MPa at 50−70 °C were conducted for 5 h. The annealing periods at 65 and 70 °C were 300 and 50 h, respectively. q is the scattering vector, defined by $q = (4\pi n/\lambda)\sin(\theta/2)$. Average spherulite radius R is calculated from $R = 4.09/q$.

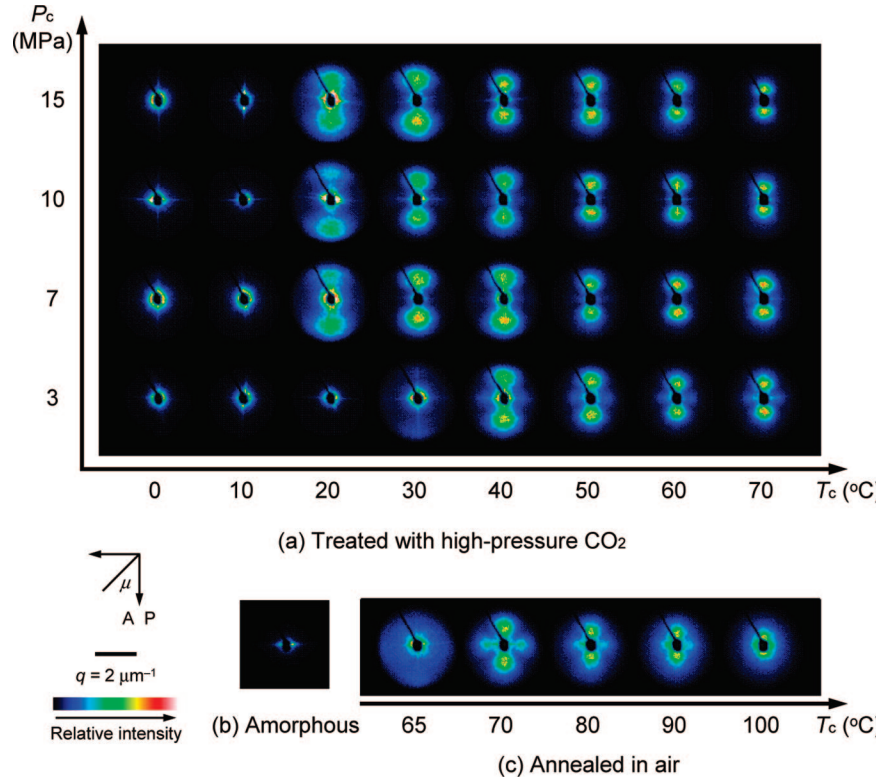

Figure 9. Vv light scattering patterns of the CO_2-treated films and annealed ones. The CO_2 treatments under 3−15 MPa at 0−40 °C and annealing in air at 80−100 °C were conducted for 2 h. The CO_2 treatments under 3−15 MPa at 50−70 °C were conducted for 5 h. The annealing periods at 65 and 70 °C were 300 and 50 h, respectively.

decreasing CO_2 treatment temperature. Therefore, when there is a linear relationship between the spherulite radius and T_c, the dominant parameter in determining the spherulite size should be the degree of supercooling, not the chain mobility. Namely, it is indicated that the size of spherulite formed under high-pressure CO_2 is determined by the degree of supercooling, as is the case with the crystallization in air. In addition, at the same T_c (70 °C), the spherulite radius of the CO_2-treated PLLA was

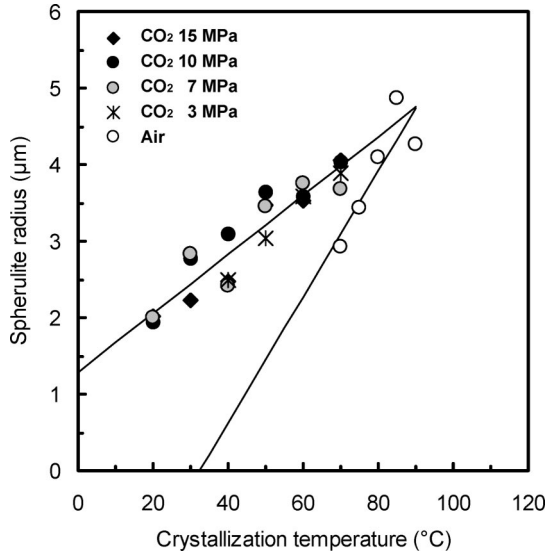

Figure 10. Average spherulite radius of the CO_2-treated films and annealed ones as functions of crystallization temperature and pressure. The CO_2 treatments under 3−15 MPa at 0−40 °C and annealing in air at 80−90 °C were conducted for 2 h. The CO_2 treatments under 3−15 MPa at 50−70 °C were conducted for 5 h. The annealing periods at 70 and 75 °C were 50 and 10 h, respectively.

larger than that of the annealed one. Since these CO_2-treated films and the annealed one showed the equivalent χ_{c_DSC} (44−50%), as shown in Figure 6, it follows that the number of crystal nuclei formed under high-pressure CO_2 is smaller than that formed in air at the same temperature. This result can be explained by the CO_2-induced depression in the degree of supercooling.[25−27]

On the other hand, in the case of the high-pressure CO_2 treatments under 7−15 MPa at 0−10 °C, those under 3 MPa at 0−30 °C, and the annealing in air at 65 °C, Hv light scattering was not the "four-leaf-clover" pattern. The films crystallized under 7−15 MPa CO_2 at 0−10 °C and those crystallized under 3 MPa CO_2 at 10−20 °C showed the scattering streaks in horizontal and vertical directions (described as the "+-type pattern"), while that crystallized under 3 MPa CO_2 at 0 °C gave rise to the scattering streaks at azimuthal angle of odd multiples of 45° (described as the "×-type pattern"). Vv light scattering of these CO_2-treated films showing the "+-type Hv pattern" or "×-type Hv pattern" had almost no azimuthal angle dependence, (i.e., circularly symmetric pattern). Such combinatorial light scattering patterns in Hv and Vv polarization for these CO_2-treated PLLA films are comparable with those for the collagen films, reported by Moritani et al.[34] They explained the light scattering patterns of the collagen films in the air-dried state using the random assembly model of anisotropic rods in three dimensions, which was obtained by extending the two-dimensional rod model proposed by Samuels[35] and Rhodes and Stein.[36] In the rod model, the principal axis of the polarizability ellipsoids of the scattering elements within the rod is tilted at a given polar angle, ω_0, to the long axis of the rod.[30,34−36] This polar angle (ω_0) is the dominant parameter that determines the μ dependence of the light scattering pattern. When ω_0 is around 45°, the calculated Hv scattering pattern shows the "+-type feature", which corresponds to the PLLA crystallized under 7−15 MPa CO_2 at 0−10 °C or under 3 MPa CO_2 at 10−20 °C. In contrast, when ω_0 is 0 or 90°, the calculated Hv scattering pattern becomes the "×-type pattern", which corresponds to the PLLA crystallized under 3 MPa CO_2 at 0 °C. With increasing CO_2 treatment pressure or temperature, the "×-type pattern" changed to the "+-type pattern", indicating the change in ω_0 with the CO_2 pressure or temperature. The random assembly model of anisotropic plates with tilted scattering elements gives qualitatively equal Hv light scattering patterns to those of anisotropic rods.[37] Also, the random assembly model of sheaflike textures having a small sector (fan) angle, which corresponds to the random assembly of rodlike superstructures, gives the similar Hv scattering to the "+-type Hv scattering", although the scattering peaks exist at a given θ unlike the "+-type scattering".[30,38,39]

The film crystallized in air at 65 °C yielded the broad scattering streaks in horizontal and vertical directions (described as the "*broad*-+-type pattern"). In Vv polarization, this annealed film showed the circularly symmetric scattering. Such "*broad*-+-type Hv pattern" and the circularly symmetric Vv one indicate that the formation of rodlike superstructures with the disorder in arrangement of crystallites occurs by the crystallization in air just above T_g. The low chain mobility of PLLA in air at 65 °C (just above T_g, i.e., the diffusion-controlled region) should be linked with the disorder in arrangement of crystallites within rodlike superstructures.

For the film treated with CO_2 under 3 MPa at 30 °C, Hv scattering similar to the "four-leaf-clover" pattern (spherulites) was observed, although the scattering peaks were much broader compared with those of the "four-leaf-clover" pattern and simultaneously the "+-type pattern" (rodlike superstructures) was observed in small-angle region. The corresponding Vv light scattering was the mixture of the circularly symmetric scattering in small-angle region (rodlike superstructures) and the broad scattering in vertical direction in wide-angle region (spherulites). These combinatorial light scattering patterns indicate that the rodlike superstructures, sheaflike ones, and spherulites are formed under 3 MPa CO_2 at 30 °C. Namely, 30 °C is the morphological transition temperature under 3 MPa CO_2. In contrast, the transition temperature from the "four-leaf-clover" Hv pattern to the "+-type Hv pattern" was around 15 °C for the CO_2 treatments under 7−15 MPa. Thus, it was clarified that the morphological transition temperature decreases with the CO_2 pressure, which can be explained by the increase in the chain mobility due to the CO_2-enhanced T_g depression, and the decrease in the crystal nucleation density due to the enhancement of T_m depression with the CO_2 pressure.

In summary, light scattering studies revealed that the spherulite size decreases with decreasing CO_2 treatment temperature regardless of the CO_2 pressure, and the morphological transition from spherulites to rodlike crystalline superstructures occurs around 15 °C under 7−15 MPa CO_2 and around 30 °C under 3 MPa CO_2. Thus, it was clarified that the dominant factor that determines the crystalline morphology of PLLA is the CO_2 treatment temperature, as is the case with the crystalline structure (the $\alpha''-\alpha$ transition).

Although both the CO_2-treated PLLA films (under 7−15 MPa at 20−70 °C and under 3 MPa at 40−70 °C) and annealed ones (70−120 °C) were confirmed to have spherulites, there was a clear difference in their Vv light scattering patterns. These CO_2-treated films showed only the two-point scattering pattern in vertical direction, while the annealed ones (70−120 °C) showed not only the vertical two-point scattering pattern but also the horizontal scattering streak, as shown in Figure 9. Furthermore, it should be noted that the Vv light scattering feature of the CO_2-treated PLLA (two-point scattering) showed almost no change with the CO_2 treatment temperature, although the crystalline structure of PLLA had a strong dependence on the CO_2 treatment temperature, as shown in Figures 3, 4, and 5. Here, the theoretical Vv light scattering intensity from the perfect spherulites (I_{Vv_sph}) is given by[30−33]

$$I_{Vv\_sph} = AV_0^2 \cos^2 \rho_1 (3/U^3)^2 \{(\alpha_r - \alpha_s)(SiU - \sin U) + (\alpha_t - \alpha_s)(2 \sin U - U \cos U - SiU) + (\alpha_r - \alpha_t)[\cos^2(\theta/2)/\cos \theta] \cos^2 \mu (4 \sin U - U \cos U - 3SiU)\}^2 \quad (5)$$

$$\cos \rho_1 = \frac{\cos \theta}{\sqrt{\cos^2 \theta + \sin^2 \theta \cos^2 \mu}} \quad (6)$$

$$SiU = \int_0^U \frac{\sin x}{x} dx \quad (7)$$

$$U = \frac{4\pi R}{\lambda'} \sin\left(\frac{\theta}{2}\right) \quad (8)$$

where A is a proportional constant; V_0 is the volume of the spherulite ($= 4\pi R^3/3$); cos ρ_1 is the geometric polarization correction term, which distorts the Vv light scattering pattern in horizontal direction; α_r and α_t are the radial and tangential polarizabilities of the spherulite, respectively; α_s is the polarizability of the surroundings; SiU is the sine integral of U; θ is a scattering angle; μ is a azimuthal angle; R is the radius of the spherulite; and λ' is the wavelength of light in the medium ($= \lambda/n$, where n is the refractive index of the medium). In eq 5, the first term $(\alpha_r - \alpha_s)(SiU - \sin U)$ and second term $(\alpha_t - \alpha_s)(2 \sin U - U \cos U - SiU)$ have no μ dependence (i.e., depend only on θ). In contrast, the third term $(\alpha_r - \alpha_t)[\cos^2(\theta/2)/\cos \theta] \cos^2 \mu (4 \sin U - U \cos U - 3SiU)$ has the μ dependence as well as θ dependence. The Vv light scattering pattern is determined mainly by the magnitude and sign of these three terms. When R is given, the magnitude and sign of the polarizability weighing coefficients for these three terms—$(\alpha_r - \alpha_s)$, $(\alpha_t - \alpha_s)$, and $(\alpha_r - \alpha_t)$—determine the Vv light scattering pattern. Since there are many combinations of α_r, α_t, and α_s yielding the equivalent Vv light scattering patterns, another expression of the polarizability weighing coefficients is proposed as follows. In the crystalline/amorphous two-phase system with $\alpha_r < \alpha_t$, which corresponds to negative birefringent spherulites such as PLLA,[8,13−15] the fluctuation in density (η) and that in optical anisotropy (Δ) are given by[30]

$$\eta = v(\alpha_c - \alpha_a) = v(\alpha_c - \alpha_s) \quad (9)$$

$$\Delta = v(\alpha_{||} - \alpha_\perp) = v(\alpha_t - \alpha_r) \quad (10)$$

$$\alpha_c = \frac{\alpha_{||} + 2\alpha_\perp}{3} = \frac{\alpha_t + 2\alpha_r}{3} \quad (11)$$

where v is the fluctuation in the local crystalline volume fraction; α_c is the mean polarizability of the crystalline phase; α_a is the polarizability of the amorphous phase, which was set equal to α_s in eq 5; $\alpha_{||}$ is the polarizability parallel to the optically principal axis of crystallites within crystalline superstructure like spherulite, which was set equal to α_t in eq 5; and $\alpha_\perp$ is the polarizability perpendicular to the optically principal axis of crystallites within crystalline superstructure, which was set equal to α_r in eq 5. From eqs 5, 9, 10, and 11, I_{Vv_sph} can be rewritten as

$$I_{Vv\_sph} = A(\Delta/v)^2 V_0^2 \cos^2 \rho_1 (3/U^3)^2 \{(\eta/\Delta - 1/3)(SiU - \sin U) + (\eta/\Delta + 2/3)(2 \sin U - U \cos U - SiU) - [\cos^2(\theta/2)/\cos \theta] \cos^2 \mu (4 \sin U - U \cos U - 3SiU)\}^2 \quad (12)$$

In eq 12, if the constant Δ/v is given, the Vv light scattering intensity can be determined by η. When Δ/v is not constant, the Vv light scattering intensity cannot be determined by η, but its feature (e.g., two-point scattering feature) can be determined by the one parameter, η/Δ. In other words, $I_{Vv\_sph}/[A(\Delta/v)^2]$ can be obtained by η/Δ. Figure 11 displays the η/Δ dependence of $I_{Vv\_sph}/[A(\Delta/v)^2]$. As can be seen, the azimuthal-angle dependence of $I_{Vv\_sph}/[A(\Delta/v)^2]$ changes continuously with increasing η/Δ. When η/Δ is in the range from −0.45 to −0.40, the corresponding Vv light scattering feature is comparable with that of the annealed PLLA films. When η/Δ is in the range from −0.30 to −0.20, the calculated Vv light scattering feature is in agreement with that of the CO_2-treated films having spherulites. Thus, the theoretical calculations show that η/Δ of the CO_2-treated films that have spherulites is different from that of the annealed ones (70−120 °C). Here, for a better understanding of the meaning of difference in η/Δ, the relationship among α_r, α_t, α_s, and η/Δ is obtained from eqs 910−11:

$$\alpha_s = (2/3 + \eta/\Delta)\alpha_r + (1/3 - \eta/\Delta)\alpha_t \quad (13)$$

$$(\alpha_t - \alpha_s)/\Delta = 2/3 + \eta/\Delta \quad (14)$$

$$(\alpha_s - \alpha_r)/\Delta = 1/3 - \eta/\Delta \quad (15)$$

Equation 13 means that the relationship among α_r, α_t, and α_s can be given by η/Δ. In addition, eqs 14 and 15 show that $(\alpha_t - \alpha_s)/\Delta$ increases and $(\alpha_s - \alpha_r)/\Delta$ decreases with increasing η/Δ. Because η/Δ of the CO_2-treated PLLA is larger than that of the annealed one, it follows that $(\alpha_t - \alpha_s)/\Delta$ of the former is larger than that of the latter, and $(\alpha_s - \alpha_r)/\Delta$ of the former is smaller than that of the latter. These results indicate that there is a difference in the arrangement of crystalline lamellae within spherulite between the CO_2-treated films and annealed ones. Thus, it was found that CO_2 has a strong effect on the arrangement of crystallites within spherulite as well as the crystalline structure for PLLA. Oda, Koga, and Saito showed that the order of spherulite formed under CO_2 is much lower than that formed in air by in situ light scattering and optical microscopy measurements.[28,42] They pointed out that such disorder in spherulites formed under CO_2 is due to the exclusion of CO_2 from the crystalline region. Such a CO_2 exclusion effect should be responsible for the changes in the arrangement of

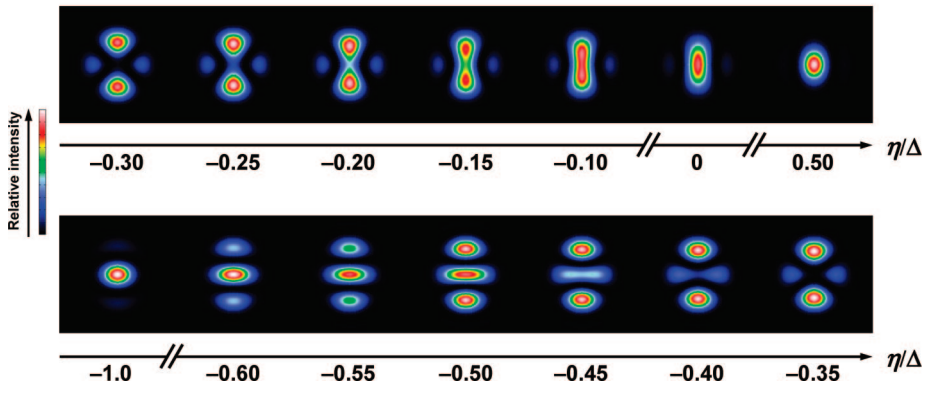

Figure 11. η/Δ dependence of the theoretical Vv light scattering patterns from perfect spherulites.

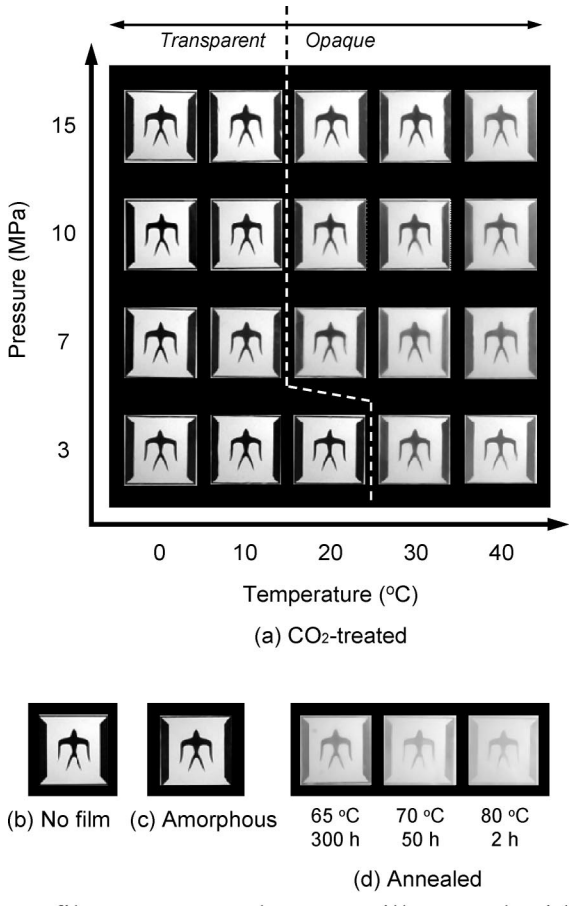

Figure 12. Photographs of PLLA films put over the paper illustrated with a symbol for showing the transparency of a film: (a) CO_2-treated films, (b) no film, (c) amorphous one, and (d) annealed ones. The CO_2 treatments under 3−15 MPa at 0−40 °C were conducted for 2 h.

crystallites within spherulite (the changes in η/Δ) as well as the structural distortion on the unit cell scale (the α'' form) for PLLA.

Transparency of CO_2-Treated PLLA Films. The photographs of the CO_2-treated PLLA films compared with those of the amorphous one and annealed ones are shown in Figure 12. The films treated with CO_2 at 0−10 °C under 7−15 MPa and those crystallized at 0−20 °C under 3 MPa CO_2 exhibited the transparency comparable with that of the amorphous one, indicating that the size of crystalline superstructure in these CO_2-treated films is smaller than the wavelength of the visible light (i.e., on a nanometer scale).[24] Interestingly, the formation of rodlike crystalline superstructures (the "+-type Hv pattern" and "×-type Hv pattern") was clarified under these CO_2 treatment conditions. Therefore, it follows that the rodlike superstructures on a nanometer scale are dispersed homogeneously in these films. On the contrary, the films were opaque for the CO_2 treatments under 7−15 MPa at 20−70 °C, those under 3 MPa at 30−70 °C, and the annealing in air at 65−140 °C. The formation of spherulites on a micrometer scale, as shown in Figure 10, is responsible for the opaqueness of a film for the CO_2 treatments under 7−15 MPa at 20−70 °C, those under 3 MPa at 30−70 °C, and the annealing in air at 70−120 °C, although the rodlike superstructures as well as spherulites are formed under 3 MPa CO_2 at 30 °C. The film crystallized in air at 65 °C, which showed the "*broad*-+-type Hv pattern", became opaque, indicating the formation of the rodlike superstructures on a micrometer scale.

The CO_2-treated PLLA films started to be clouded when treated with CO_2 at 20 °C under 7−15 MPa and at 30 °C under 3 MPa, and the transparency of a film decreased with increasing T_c. This result agrees with the trend of change in the spherulite radius with temperature (i.e., the transparency of a film decreased with increasing the size of spherulite). Similarly, for the annealed films, the transparency of a film decreased with increasing T_c. Thus, the increase in the spherulite size is responsible for the decrease in the film transparency for both the CO_2 treatment and annealing in air. Here, it should be noted that there was a difference in the film transparency between the CO_2-treated films and annealed ones having the equivalent radius of spherulite. For example, the transparency of the CO_2-treated films (30 °C and 7−10 MPa) was obviously higher than that of the annealed one (70 °C), although the spherulite radius of the former (2.8 μm) was comparable with that of the latter (2.9 μm), as shown in Figure 10. As mentioned above, the results of light scattering suggest that the arrangement of crystallites within spherulite formed under high-pressure CO_2 is different from that formed in air. Accordingly, the difference in the arrangement of crystallites within spherulite might be linked with the difference in the transparency between the CO_2-treated films and annealed ones having the equivalent spherulite radius.

There was a clear difference in the transparency of a film among the films having nonspherulitic crystalline superstructures. The films showing the "+-type Hv pattern" and "×-type Hv pattern" exhibited the transparency comparable with that of the amorphous one, whereas the film showing the "*broad*-+-type Hv pattern" was clouded as is the case with the films having spherulites on a micrometer scale. Therefore, the formation of the nonspherulitic superstructures is not necessarily correlated with the transparency equivalent to that of the amorphous film.

Figure 13 is the schematic illustration describing the CO_2 pressure and temperature dependence of the crystalline superstructures of PLLA formed under high-pressure CO_2 compared with those formed in air, which was characterized by the light scattering technique and film transparency.

Morphological Transition Mechanisms from Microsize Spherulites to Nanosize Rods. As mentioned above, light scattering studies on the CO_2-treated PLLA films revealed that the spherulite size decreases with decreasing temperature and the morphological transition from spherulites on a micrometer scale to rodlike crystalline superstructures on a submicrometer scale occurs around 15 °C under 7−15 MPa and around 30 °C under 3 MPa. First, we discuss the origin of the formation of rodlike superstructures on a nanometer scale by comparing the CO_2-treated PLLA and the annealed one in terms of the degree of supercooling. In general, the formation of a large number of crystal nuclei is triggered by a high degree of supercooling.[51] In contrast, the mobility of polymer chains decreases with decreasing temperature and main chains are frozen at T_g. Therefore, the spherulite size decreases with decreasing T_c and polymer crystallization cannot occur below T_g in spite of a high degree of supercooling. Namely, it follows that the size of crystalline superstructure has the minimum value at T_g for crystallization in air.

Under high-pressure CO_2, on the other hand, polymer chains have high enough mobility to diffuse toward a crystal growth front by the plasticizing effect of CO_2 even at the temperature below original T_g. At the same T_c, the degree of supercooling ($T_m - T_c$) for the crystallization under high-pressure CO_2 is smaller than that for the crystallization in air because of the CO_2-induced T_m depression. However, if the high-pressure CO_2treatment is conducted at a low enough temperature to have the degree of supercooling much higher than that in air at T_g, the size of the crystalline superstructure should be far smaller than that for the crystallization in air at T_g. The size of crystalline superstructure formed under 7−15 MPa CO_2 at 0−10 °C and

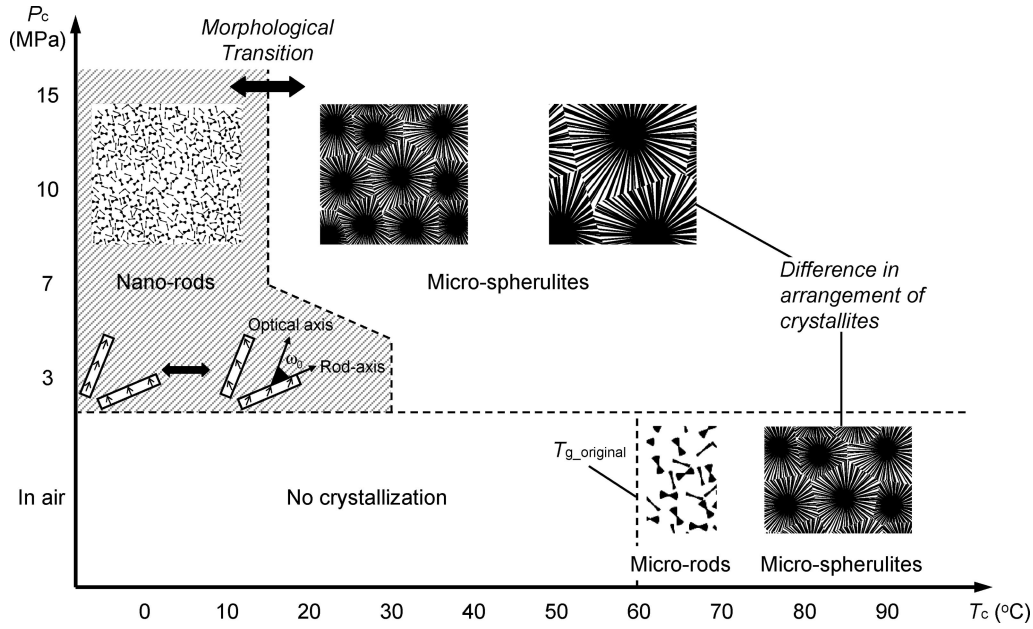

Figure 13. Schematic illustration showing the crystallization temperature (T_c) and pressure (P_c) dependence of the crystalline superstructures of the CO_2-treated PLLA and comparison with those of the annealed one.

under 3 MPa CO_2 at 0−20 °C (nanometer scale) was much smaller than that formed in air just above T_g (micrometer scale). These results indicate that under these high-pressure CO_2 conditions, the crystal nucleation density of PLLA is much higher than that in air just above T_g. Therefore, the relatively high degree of supercooling under high-pressure CO_2 below room temperature should be responsible for the formation of crystalline superstructures on a nanometer scale. Since the annealed film was opaque even by the crystallization just above T_g, 65 °C, it will be difficult to obtain the transparent crystallized films in the unoriented state by the annealing in air.

Second, we discuss the origin of the formation of rodlike crystalline superstructures on a nanometer scale in terms of morphological changes in the early stage of polymer crystallization. The "sheaflike unidirectional growth" is one of the growth mechanisms leading to spherical symmetry.[45,52−54] This spherulitic growth mechanism shows the formation of sheaflike crystals in the early stage of crystallization. Using light scattering technique, Stein and Misra characterized the evolution of poly(ethylene terephthalate) (PET) spherulites from rodlike nuclei through sheaflike crystals at the beginnings of crystallization.[55,56] They used the "fan model", in which changing the "fan angle" from near 0 to 90° yields the morphological development from rodlike precursors to perfect spherulites through sheaflike crystals.[38,39] Such morphological changes in the early stage of crystallization were confirmed not only by light scattering technique but also by microscopical observation; for example, in crystallization of polychlorotrifluoroethylene at 161 °C.[38] Lee et al. also investigated the crystalline structure evolution of PET using the time-resolved light scattering method.[57] They showed that the isotropic embryo that is a highly disordered crystalline domain with low crystallinity is formed in the early stage of crystallization and subsequently grows to be spherulite with increasing size and order. In this manner, the formation of the nonspherulitic crystalline superstructures in the early stage of crystallization has been reported by many researchers. As discussed above, it is suggested that the formation of a relatively large number of crystal nuclei is triggered by a relatively large degree of supercooling under 7−15 MPa CO_2 at 0−10 °C and under 3 MPa CO_2 at 0−20 °C. As a result, the impingement of the neighboring crystalline superstructures should occur in the early stage of crystallization, which prevents the rodlike crystalline superstructures from growing to be spherulites.

Conclusions

Crystalline structure and morphology of PLLA formed under CO_2 under various pressure and temperature conditions were characterized by comparing the CO_2-treated PLLA and the annealed one in terms of the crystallization behavior, crystalline forms, and crystalline superstructures. The CO_2-induced crystallization at the temperature lower than original T_g of PLLA was revealed by DSC and WAXD measurements. The T_c dependence of the diffraction peak position ($2\theta \approx 16°$) and crystallinity for the CO_2-treated PLLA indicates that the crystals formed under high-pressure CO_2 are disordered and have poor chain packing compared with those formed in air and the crystal modification changes from disorder α (α″) to α forms not through the α′ one with increasing CO_2 treatment temperature. It was clarified that PLLA molecules form the α″ crystals under 3−15 MPa CO_2 at 0−20 °C and under 7−15 MPa CO_2 at 30 °C, whereas the α crystals are formed under 7−15 MPa CO_2 at 50−70 °C.

By using the light scattering technique, it was clarified that the spherulite size decreases with decreasing CO_2 treatment temperature and the morphological transition from spherulites on a micrometer scale to rodlike crystalline superstructures on a nanometer scale occurs around 15 °C under 7−15 MPa and around 30 °C under 3 MPa. The high transparency of the CO_2-treated PLLA films (under 7−15 MPa at 0−10 °C and under 3 MPa at 0−20 °C) is due to the formation of rodlike superstructures on a nanometer scale. It was found that the CO_2 treatment temperature is the dominant factor that determines the crystalline structure and morphology of PLLA. Furthermore, by introducing the parameters η (the fluctuation in density) and Δ (the fluctuation in optical anisotropy) to the theoretical equation for Vv light scattering from the perfect spherulites, the relative intensity $I_{Vv\_sph}/[A(\Delta/\nu)^2]$ can be determined by the one parameter η/Δ. The difference in η/Δ between the CO_2-treated films and annealed ones indicates that there is a difference in the arrangement of crystallites within spherulite between these films. Namely, it was demonstrated that CO_2 has a strong effect on the arrangement of crystallites within spherulite (the changes in η/Δ) as well as the chain packing in the unit cell (the α″

form) and size of the crystalline superstructure (the rodlike superstructures on nanometer scale) for PLLA.

Acknowledgment. We thank Dr. Y. Tominaga (Tokyo University of Agriculture and Technology), Dr. H. Shii (Tokyo Institute of Technology), and Dr. K. Kuboyama (Tokyo Institute of Technology) for giving us beneficial suggestions and comments. We also thank the Toyota Motor Corporation, Japan, for supplying the PLLA pellets.

References and Notes

(1) Santis, P. D.; Kovacs, A. J. *Biopolymers* **1968**, *6*, 299–306.
(2) Hoogsteen, W.; Postema, A. R.; Pennings, A. J.; ten Brinke, G.; Zugenmaier, P. *Macromolecules* **1990**, *23*, 634–642.
(3) Eling, B.; Gogolewski, S.; Pennings, A. J. *Polymer* **1982**, *23*, 1587–1593.
(4) Cartier, L.; Okihara, T.; Ikada, Y.; Tsuji, H.; Puiggali, J.; Lotz, B. *Polymer* **2000**, *41*, 8909–8919.
(5) Zhang, J.; Duan, Y.; Sato, H.; Tsuji, H.; Noda, I.; Yan, S.; Ozaki, Y. *Macromolecules* **2005**, *38*, 8012–8021.
(6) Zhang, J.; Tashiro, K.; Domb, A. J.; Tsuji, H. *Macromol. Symp.* **2006**, *242*, 274–278.
(7) Zhang, J.; Tashiro, K.; Tsuji, H.; Domb, A. J. *Macromolecules* **2008**, *41*, 1352–1357.
(8) Cho, T. Y.; Strobl, G. *Polymer* **2006**, *47*, 1036–1043.
(9) Kawai, T.; Rahman, N.; Matsuba, G.; Nishida, K.; Kanaya, T.; Nakano, M.; Okamoto, H.; Kawada, J.; Usuki, A.; Honma, N.; Nakajima, K.; Matsuda, M. *Macromolecules* **2007**, *40*, 9463–9469.
(10) Pan, P.; Kai, W.; Zhu, B.; Dong, T.; Inoue, Y. *Macromolecules* **2007**, *40*, 6898–6905.
(11) Pan, P.; Zhu, B.; Kai, W.; Dong, T.; Inoue, Y. *J. Appl. Polym. Sci.* **2008**, *107*, 54–62.
(12) Yasuniwa, M.; Sakamo, K.; Ono, Y.; Kawahara, W. *Polymer* **2008**, *49*, 1943–1951.
(13) Kalb, B.; Pennings, A. J. *Polymer* **1980**, *21*, 607–612.
(14) Vasanthakumari, R.; Pennings, A. J. *Polymer* **1983**, *24*, 175–178.
(15) Yasuniwa, M.; Tsubakihara, S.; Iura, K.; Ono, Y.; Dan, Y.; Takahashi, K. *Polymer* **2006**, *47*, 7554–7563.
(16) Tomasko, D. L.; Li, H.; Liu, D.; Han, X.; Wingert, M. J.; Lee, L. J.; Koelling, K. W. *Ind. Eng. Chem. Res.* **2003**, *42*, 6431–6456.
(17) Condo, P. D.; Sanchez, I. C.; Panayiotou, C. G.; Johnston, K. P. *Macromolecules* **1992**, *25*, 6119–6127.
(18) Zhang, Z.; Handa, Y. P. *Macromolecules* **1997**, *30*, 8505–8507.
(19) Chow, T. S. *Macromolecules* **1980**, *13*, 362–364.
(20) Chiou, J. S.; Barlow, J. W.; Paul, D. R. *J. Appl. Polym. Sci.* **1985**, *30*, 3911–3924.
(21) Mizoguchi, K.; Hirose, T.; Naito, Y.; Kamiya, Y. *Polymer* **1987**, *28*, 1298–1302.
(22) Handa, Y. P.; Zhang, Z.; Wong, B. *Macromolecules* **1997**, *30*, 8499–8504.
(23) Asai, S.; Shimada, Y.; Tominaga, Y.; Sumita, M. *Macromolecules* **2005**, *38*, 6544–6550.
(24) Hirota, S.; Sato, T.; Tominaga, Y.; Asai, S.; Sumita, M. *Polymer* **2006**, *47*, 3954–3960.
(25) Takada, M.; Ohshima, M. *Polym. Eng. Sci.* **2003**, *43*, 479–489.
(26) Takada, M.; Tanigaki, M.; Ohshima, M. *Polym. Eng. Sci.* **2001**, *41*, 1938–1946.
(27) Takada, M.; Hasegawa, S.; Ohshima, M. *Polym. Eng. Sci.* **2004**, *44*, 186–196.
(28) Oda, T.; Saito, H. *J. Polym. Sci., Part B: Polym. Phys.* **2004**, *42*, 1565–1572.
(29) Teramoto, G.; Oda, T.; Saito, H.; Sano, H.; Fujita, Y. *J. Polym. Sci., Part B: Polym. Phys.* **2004**, *42*, 2738–2746.
(30) Haudin, J. M. In *Optical Properties of Polymers*; Meeten, G. H., Ed.; Elsevier Applied Science Publishers: London, 1986; pp 167−264.
(31) Stein, R. S.; Rhodes, M. B. *J. Appl. Phys.* **1960**, *31*, 1873–1884.
(32) Samuels, R. J. *J. Polym. Sci., Part A-2* **1971**, *9*, 2165–2246.
(33) Samuels, R. J. *J. Polym. Sci., Polym. Phys. Ed.* **1974**, *12*, 1417–1439.
(34) Moritani, M.; Hayashi, N.; Utsuo, A.; Kawai, H. *Polym. J.* **1971**, *2*, 74–87.
(35) Samuels, R. J. *J. Polym. Sci., Part A-2* **1969**, *7*, 1197–1258.
(36) Rhodes, M. B.; Stein, R. S. *J. Polym. Sci, Part A-2* **1969**, *7*, 1539–1558.
(37) Matsuo, M.; Nomura, S.; Hashimoto, T.; Kawai, H. *Polym. J.* **1974**, *6*, 151–164.
(38) Picot, C.; Stein, R. S.; Motegi, M.; Kawai, H. *J. Polym. Sci., Part A-2* **1970**, *8*, 2115–2126.
(39) Motegi, M.; Oda, T.; Moritani, M.; Kawai, H. *Polym. J.* **1970**, *1*, 209–221.
(40) Yasuniwa, M.; Iura, K.; Dan, Y. *Polymer* **2007**, *48*, 5398–5407.
(41) Rosa, C. D.; Guerra, G.; Petraccone, V.; Pirozzi, B. *Macromolecules* **1997**, *30*, 4147–4152.
(42) Koga, Y.; Saito, H. *Polymer* **2006**, *47*, 7564–7571.
(43) Keith, H. D. In *Physics and Chemistry of the Organic Solid State*; Fox, D., Labes, M. M., Weissberger, A., Eds.; Interscience Publishers: New York, 1963; Vol. *1*, pp 462−542.
(44) Dole, M. *J. Polym. Sci., Part C* **1967**, *18*, 57–68.
(45) Wunderlich, B. *Macromolecular Physics*; Academic Press: New York, 1973; Vol. *1*.
(46) Fischer, E. W.; Sterzel, H. J.; Wegner, G. *Kolloid Z. Z. Polym.* **1973**, *251*, 980–990.
(47) Iannace, S.; Nicolais, L. *J. Appl. Polym. Sci.* **1997**, *64*, 911–919.
(48) Sarasua, J. R.; Prud'homme, R. E.; Wisniewski, M.; Borgne, A. L.; Spassky, N. *Macromolecules* **1998**, *31*, 3895–3905.
(49) Cohn, D.; Younes, H.; Marom, G. *Polymer* **1987**, *28*, 2018–2022.
(50) Hoffman, J. D.; Weeks, J. J. *J. Res. Natl. Bur. Stand. (U.S.)* **1962**, *66A*, 13–28.
(51) Mandelkern, L. *Crystallization of Polymers*, 2nd ed.; Cambridge University Press: Cambridge, 2004; Vol. *2*.
(52) Bodor, G. *Structural Investigation of Polymers*; Kemp, T. J., Kennedy, J. F., Eds.; Ellis Horwood Series in Polymer Science and Technology; Ellis Horwood: Chichester, 1991.
(53) Keith, H. D.; Padden, F. J. *J. Appl. Phys.* **1963**, *34*, 2409–2421.
(54) Norton, D. R.; Keller, A. *Polymer* **1985**, *26*, 704–716.
(55) Misra, A.; Stein, R. S. *J. Polym. Sci., Part B* **1972**, *10*, 473–477.
(56) Stein, R. S.; Misra, A. *J. Polym. Sci., Polym. Phys. Ed.* **1973**, *11*, 109–116.
(57) Lee, C. H.; Saito, H.; Inoue, T. *Macromolecules* **1993**, *26*, 6566–6569.

MA800766H